AIChE

# Light FCC Gasoline Olefin Oligomerization over a Magnetic $NiSO_4/\gamma$-$Al_2O_3$ Catalyst in a Magnetically Stabilized Bed

**Ying Peng, Minghui Dong, Xiangkun Meng, and Baoning Zong**
State Key Laboratory of Catalytic Materials and Reaction Engineering, Research Institute of Petroleum Processing, SINOPEC, Beijing 100083, P.R. China

**Jinli Zhang**
School of Chemical Engineering and Technology, Tianjin University, Tianjin 300072, P.R. China

*DOI 10.1002/aic.11712*
*Published online February 4, 2009 in Wiley InterScience (www.interscience.wiley.com).*

*Magnetic $NiSO_4/\gamma$-$Al_2O_3$ catalysts were prepared by impregnating $NiSO_4$ solutions onto the $\gamma$-$Al_2O_3$ support containing a magnetic material of $Fe_3O_4$. Characterization by XRD, $NH_3$-TPD, and thermal analysis showed that the magnetic $NiSO_4/\gamma$-$Al_2O_3$ catalyst with a nickel content of 7.0% by weight had a monolayer dispersion of $NiSO_4$ and the largest number of moderate strength acid sites, and a high specific saturation magnetization. The magnetic catalyst was evaluated for light FCC gasoline olefin oligomerization in both fixed-bed and magnetically stabilized bed (MSB) reactors. Comparing with that in the fixed-bed reactor, the optimal reaction temperature in the MSB lowered to 443 K, and its space velocity ranged broadly from 2.0 to 6.0 $h^{-1}$. The sulfur-free diesel distillate produced by operation of the MSB for 100 h had higher cetane number and good low-temperature flow property, which illuminates a promising application of the MSB to manufacture clean diesel fuels with high productivity and flexibility*. © 2009 American Institute of Chemical Engineers *AIChE J,* 55: 717–725, 2009
*Keywords: magnetic solid acid catalyst, clean diesel, olefin oligomerization, magnetically stabilized bed, process intensification*

## Introduction

It is forecast that the world will face significant diesel and naphtha deficits by 2015, not least because of the rapid increase in demand for diesel in China.[1,2] Furthermore, increasingly strict environmental protection regulations require high-quality diesel fuels. The traditional process for producing clean diesel fuels is hydrogenation; it is, however, hard for traditional hydrogenation processes to meet all the requirements for high-quality clean diesel fuels.[3]

Olefin oligomerization is a promising approach for the production of clean diesel fractions free of sulfur and aromatics.[4–7] Tabak et al. has developed an olefin oligomerization process MOGD,[8,9] which used ZSM-5 zeolites to convert light olefins($C_3$–$C_6$) to gasoline and diesel fuel in fixed-bed reactors and found that high-quality diesel was favorably produced at lower temperature (473–573 K) and higher pressure (3.0–10.0 MPa). Vaccari et al. investigated $C_2$, $C_4$, and $C_5$ olefins oligomerization over MCM-41 type catalysts for the synthesis of clean diesel fuels in a fixed-bed microreactor, and obtained high selectivity of diesel fractions from $C_4$ and $C_5$ olefins at temperatures of 413–453 K, a pressure of

Additional Supporting Information may be found in the online version of this article.

Correspondence concerning this article should be addressed to B. Zong at zongbn@ripp-sinopec.com.

5.0 MPa and weight hourly space velocities of 5.3–10.6 $h^{-1}$.[4] These previous reports on olefin oligomerization to diesel generally adopted one pure compound involving $C_4$, $C_5$ olefin as the raw material. Therefore light FCC gasoline, an industrially available stream containing large amount of olefins mixture from $C_4$ to $C_6$, is a promising raw material for oligomerization to produce clean diesel.

Solid acid catalysts such as zeolites,[8–12] aluminosilicates[13,14] and solid phosphoric acid catalysts[15,16] are all effective catalysts for the olefin oligomerization reaction. Some metal sulfates, including $NiSO_4$, $CuSO_4$, $Zr(SO_4)_2$, and $Ti(SO_4)_2$ can generate fairly large numbers of moderate or strongly acidic sites when calcined at 623–973 K and, especially when supported on metal oxides, exhibit excellent catalytic performances in olefin oligomerization.[17,18] Cai et al. have previously studied the oligomerization of light olefins ($C_2$–$C_4$) to give gasoline over an $NiSO_4/\gamma$-$Al_2O_3$ catalyst under the conditions of temperature of 323 K, pressure of 2.5 MPa and liquid hourly space velocity (LHSV) 1.0–2.0 $h^{-1}$ in a fixed-bed reactor[19,20] and found that very high catalytic activity for alkene oligomerization was obtained. It was shown that acid sites with moderate acid strength play an important role in alkene oligomerization. Sohn et al. have also studied the ethylene dimerization reaction over $NiSO_4/\gamma$-$Al_2O_3$ and $NiSO_4/Fe_2O_3$-$ZrO_2$ catalysts in a fixed bed,[21–24] and found that both catalysts exhibited good performance for ethylene dimerization at around room temperature, and that catalyst activity was closely related to its acidity. Because $NiSO_4/\gamma$-$Al_2O_3$ catalysts show such excellent olefin oligomerization performance, they can be considered as potential catalysts for the production of clean diesel through oligomerization.

The fixed-bed reactor is the typical reactor for heterogeneous catalysis in the chemical industry. Fixed-bed reactors suffer from poor heat transfer characteristics, which in the case of an exothermic reaction, such as olefin oligomerization, can lead to 'hot spots' which adversely affect the operation of the catalyst. A fixed-bed reactor also suffers from other inherent disadvantages such as limited mass transfer properties, relatively high pressure drops, and lack of operational flexibility. A magnetically stabilized bed (MSB) reactor, has the advantages of efficient interphase mass and heat transfer properties, and low pressure drop,[25–29] and has been shown to be an effective way of achieving process intensification in the purification of caprolactam[30] and the methanation of carbon monoxide[31] over Ni alloy catalysts and in the acetylene hydrogenation over Pd-supported catalysts with a magnetic material of $NiFe_2O_4$.[32] Clearly the preparation of strongly magnetic catalysts is a prerequisite if they are to be employed in an MSB reactor. Recently, magnetic solid acid catalysts with a particle diameter of less than 150 nm, have been prepared by coprecipitation of catalytic materials (e.g. $TiO_2$ or $ZrO_2$) and magnetic materials (e.g. $Fe_3O_4$ or $\gamma$-$Fe_2O_3$).[33,34] These magnetic catalysts had specific saturation magnetization of less than 12.0 emu $g^{-1}$, and are usually used as heterogeneous catalysts in a batch process, using a magnetic field to separate the catalyst from the product at the end of the reaction.

In this work, a novel strongly magnetic solid acid catalyst has been synthesized by impregnating a $\gamma$-$Al_2O_3$ containing a magnetic material of $Fe_3O_4$, with $NiSO_4$ solutions and has been characterized by XRD, $NH_3$-TPD, and thermal analysis. The resulting magnetic $NiSO_4/\gamma$-$Al_2O_3$ catalysts were evaluated as olefin oligomerization catalysts using a light FCC gasoline feedstock in both fixed-bed and MSB reactors, and the effects of reaction temperature, pressure, space velocity and magnetic field intensity on the diesel yield were studied.

## Experimental

### *Catalyst preparation*

$SiO_2$ is usually used to improve the dispersion and thermal stability properties of the fine magnetic materials involving $NiFe_2O_4$ and $Fe_3O_4$.[35,36] In this work, $Fe_3O_4$ coated with $SiO_2$ ranged from 1.0 to 6.0 $\mu$m in diameter was used as the magnetic material for the composite catalyst.

The $Fe_3O_4$ particles were prepared by coprecipitation method. $FeCl_2$ solution was mixed with $FeCl_3$ solution (the molar ratio of $Fe^{2+}$ to $Fe^{3+}$ equals 4.0) in a 1 l three-necked flask by vigorous mechanical stirring. The pH of the mixture was raised to 10–12 by adding NaOH solution. The mixture was subsequently aged at 323 K for 1.0 h. And then, the precipitate was washed several times with distilled water and absolute ethanol, and dried at 353 K for 2.0 h.

The magnetic $Fe_3O_4/SiO_2$ particles were prepared by the sol-gel method followed by acidification method. The sol-gel coating process was performed at atmosphere temperature. The mixture consisting of $Fe_3O_4$, absolute ethanol and tetraethyl orthosilicate was ultrasonificated for 30 min, followed by the addition of ammonium hydroxide solution in a dropwise manner with vigorous mechanical stirring. Stirring was continued for 6 h. Then, the particles were washed several times with distilled water and absolute ethanol, and dried at 353 K for 2.0 h.

The coated particles were further coated by acidification approach. The aforesaid coated particles, at a concentration of 20.0 g $l^{-1}$, were dispersed in distilled water with ultrasonic treatment for 5.0 min. The pH of the suspension was raised to 8–10 by adding dilute NaOH solution. The suspension was transferred into a 500 ml three-necked flask with vigorous mechanical stirring and heated to 358–368 K. $Na_2SiO_3$ and dilute HCl. solutions were simultaneous added to the suspension. The pH of the suspension was maintained at 8–10 by controlling the titrating speed of the HCl, while the titrating speed of $Na_2SiO_3$ was kept constant. After titration, the suspension was aged for 1.0 h and cooled to the room temperature. Then, the particles were washed several times with distilled water and absolute ethanol, dried at 353 K for 2.0 h. The resulting $Fe_3O_4/SiO_2$ particle contained 15% (wt) $SiO_2$ and its specific saturation magnetization was 60.2 emu $g^{-1}$.

This kind of magnetic $Fe_3O_4/SiO_2$ particles mixed quantitatively with a pseudo-boehmite solution containing 1.7% $HNO_3$ and after stiring for 30 min, the resulting mixture was dried for 12.0 h at 383 K in air, and subsequently calcined at 773 K for 4 h to afford the magnetic $\gamma$-$Al_2O_3$ support. This prepared magnetic $Al_2O_3$ support consisted of 30% (wt) magnetic material ($Fe_3O_4/SiO_2$), and was sieved in the range of 75–105 $\mu$m for further characterization. The resulting support showed a specific surface area of 195 $m^2$ $g^{-1}$.

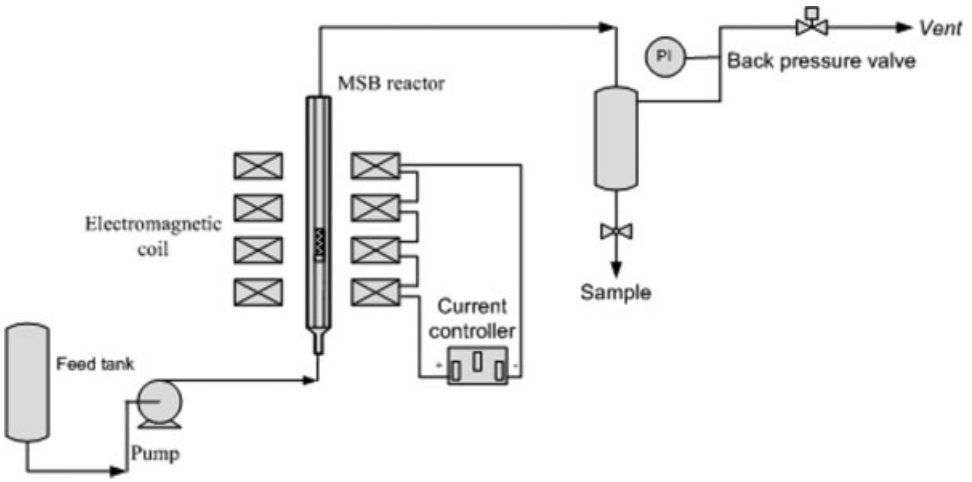


**Figure 1. Schematic diagram of the magnetically stabilized bed (MSB) experimental apparatus.**

A series of magnetic $NiSO_4/\gamma\text{-}Al_2O_3$ catalysts with different nickel contents were prepared by the incipient wetness method. The magnetic $\gamma\text{-}Al_2O_3/Fe_3O_4$ support was impregnated by an aqueous solution of $NiSO_4 \cdot 6H_2O$, and then dried at 383 K for 4.0 h followed by calcination at different temperatures for 4.0 h in air. The prepared catalyst is denoted by the weight percentage of nickel, e.g. $NiSO_4/\gamma\text{-}Al_2O_3$-4 indicates that the catalyst contains 4% (wt) nickel.

### *Characterization*

Powder XRD patterns were recorded using a Philips X'Pert Pro powder X-ray diffractometer with Cu K$\alpha$ radiation, at 40 kV and 30 mA, and a scan speed of $4^\circ$ min$^{-1}$ in the $2\theta$ range 5–80°.

Specific surface areas were measured using a Micromeritics accelerated surface area and porosimetry 2010 system. Samples were outgassed at 343 K for 8.0 h before the measurements. The specific surface area was calculated using the BET method based on the $N_2$ adsorption isotherm.

Thermal analysis was carried out on a TA Instruments Modulated DSC 2910 instrument in flowing air with a heating rate of 283 K min$^{-1}$.

Sample acidity was measured by ammonia temperature-programmed desorption (TPD) using a Micromeritics Autochem II 2920 instrument with helium as the carrier gas. Catalyst samples were allowed to adsorb $NH_3$ at 373 K, and $NH_3$ desorption was then monitored as the samples were heated to 823 K.

Magnetic properties were measured using a JDM-13 vibrating sample magnetometer manufactured by Jilin University.

Chemical composition was analyzed by Rigaku 3080 X-ray fluorescence spectrometer with rhodium target at 50 kV and 30 mA.

Elemental composition on the surface of the catalyst was measured by PekinElmer PHI Quantera SXM X-ray photoemission spectrometry (XPS) with Al K$\alpha$ radiation (sputtering conditions: argon ions with 2.0 keV energy, emission current 20 mA).

### *Evaluation of catalytic performance*

The catalytic properties of the $NiSO_4/\gamma\text{-}Al_2O_3$ materials were evaluated using the experimental apparatus shown in Figure 1. The MSB reactor, with i.d. of 9.0 mm and height of 700 mm, was surrounded by four similar DC-powered copper wire coils at regular intervals. A uniform axial magnetic field of up to 40.0 kA m$^{-1}$ can be generated in the MSB reactor by adjusting the value of the current passed through the copper coils. The loading of catalyst was 15.0 g in each run. Before feeding the hydrocarbons, the reaction system was purged for 1.0 h at room temperature by $N_2$ flow at 10.0 ml min$^{-1}$, and was then pressurized with $N_2$. The light FCC gasoline feed was then pumped into the reactor at a known flow rate.

For the purposes of comparison, the magnetic $NiSO_4/\gamma\text{-}Al_2O_3$ catalysts were also evaluated in a fixed-bed reactor having the same size as that of the MSB reactor. The fixed-bed reactor replaced the MSB reactor in the apparatus shown in Figure 1, and the treatment for each reaction run was the same as that for the MSB reactor, except for the absence of an external magnetic field.

Table 1 lists the physical properties and composition of the light FCC gasoline feed. The reaction product was separated into gasoline distillate and diesel distillate with a cutting temperature of 443 K because the amount of the distillate obtained above 623 K was less than 2.0% (wt). The per-

**Table 1. Properties of Light FCC Gasoline**

| | |
|---|---|
| Density (g/cm$^3$) | 0.643 |
| Distillation range (K) | |
| Initial boiling point | 286 |
| 10% | 299 |
| 30% | 313 |
| 50% | 329 |
| 70% | 335 |
| 90% | 347 |
| Final boiling point | 413 |
| Group composition (wt) % | |
| Saturated hydrocarbon | 50.4 |
| Olefin | 49.4 |
| Aromatic hydrocarbon | 0.2 |

formance of the catalyst was assessed by measuring the diesel yield. The properties of the product were measured after the relevant ASTM procedures.

## Results and Discussion

### *Characterization of the magnetic $NiSO_4/\gamma$-$Al_2O_3$ catalysts*

The magnetic $NiSO_4/\gamma$-$Al_2O_3$ catalysts were characterized by XRD, $NH_3$-TPD and thermal analysis, to study the influence of varying nickel content on the catalyst structure and acidity.

Figure 2a shows the XRD patterns of the magnetic $NiSO_4/\gamma$-$Al_2O_3$ catalysts with different nickel content, after calcination at 773 K for 4.0 h. When the nickel content was 7.0% (wt) or less, the only diffraction peaks observed were those characteristic of $\gamma$-$Fe_2O_3$ and $Al_2O_3$ with no peaks corresponding to $NiSO_4$. This is consistent with the formation of a monolayer of $NiSO_4$. When the nickel content was increased to 8.0% (wt), the appearance of diffraction peaks around 20 degrees $2\theta$ is consistent with the formation of crystalline $NiSO_4$ in the catalyst i.e. greater than monolayer coverage; furthermore, the intensities of these peaks increased with increasing nickel content. Cai et al. have previously reported similar results for $NiSO_4$, dispersed on a $\gamma$-$Al_2O_3$ support.[19] Furthermore, they showed that a monolayer dispersion of $NiSO_4$ exhibited high activity whereas larger loadings of $NiSO_4$, leading to the formation of double layers of $NiSO_4$, resulted in lower catalytic activity.

Figure 2b shows $NH_3$-TPD profiles of the magnetic $NiSO_4/\gamma$-$Al_2O_3$ catalysts with different nickel contents after calcination at 773 K. The $Fe_3O_4/\gamma$-$Al_2O_3$ support without any added nickel showed a strong desorption peak at about 463 K and another relatively weak peak around 593 K. As the Ni content was increased, the relative intensities of two peaks showed a gradual change i.e. the peak at higher temperature increased in intensity and its intensity exceeded that of the low temperature peak when the nickel content reached 7.0% (wt). Furthermore, the position of the high temperature peak showed a gradual shift to lower temperature with increasing nickel content, with the peak occurring around 553 K for a nickel loading of 10% (wt). It is generally accepted that a TPD peak around 463 K arises from desorption of ammonia from weak acid sites, while a peak around 553–593 K results from desorption of ammonia from moderate strength acid sites.[37] The total volume of adsorbed $NH_3$ volume increased at first with increasing nickel content, reaching a maximum at 7.0% (wt) and then decreased (see Supp. Info. Figure 1). This is consistent with the XRD patterns, since it is reasonable to assume that loadings of nickel higher than 7.0% (wt), resulting in multilayer deposition on the surface, will give partial covering of the acid sites and as a consequence the volume of adsorbed $NH_3$ will decrease.

Figure 2c shows the DTA curves of pure $NiSO_4{\cdot}6H_2O$ and the magnetic $NiSO_4/\gamma$-$Al_2O_3$ catalysts with different Ni contents. In the case of pure $NiSO_4{\cdot}6H_2O$, three endothermic peaks were observed below 673 K corresponding to dehydration of $NiSO_4{\cdot}6H_2O$, and one peak around 1153 K attributed to decomposition of $NiSO_4$.[38] The magnetic $NiSO_4/\gamma$-$Al_2O_3$ catalysts exhibited a single endothermic peak at low tempera-

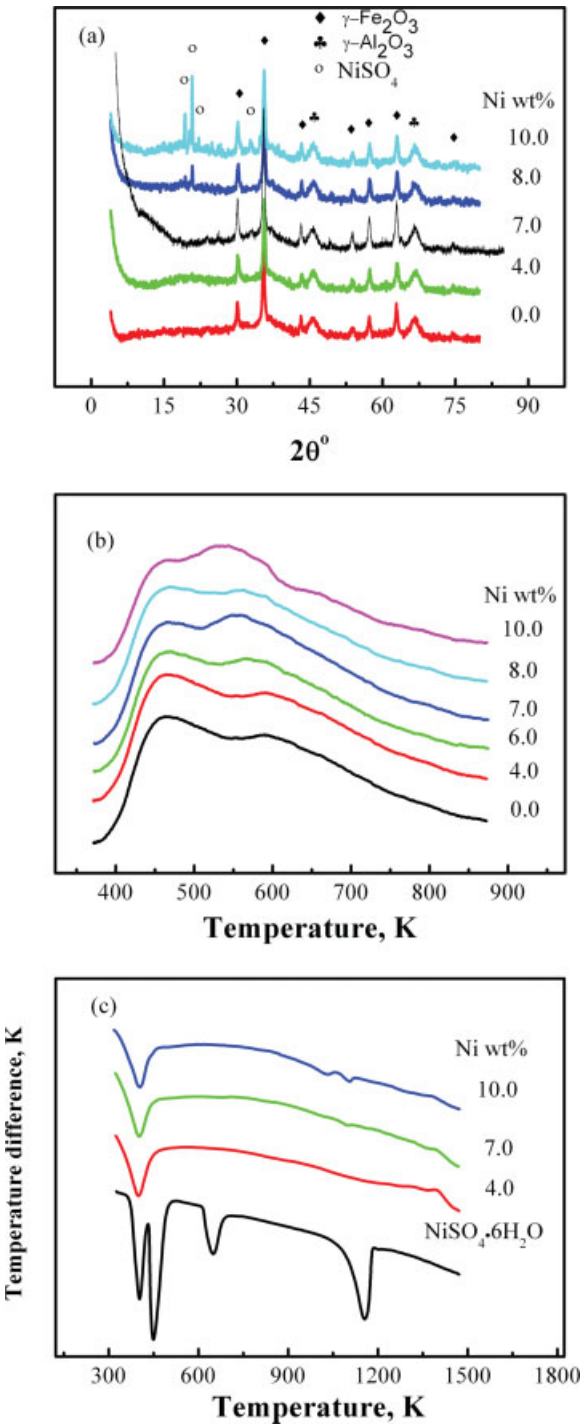


**Figure 2. (a) XRD patterns of magnetic $NiSO_4/\gamma$-$Al_2O_3$ catalysts with different nickel contents after calcination at 773 K; (b) $NH_3$-TPD curves of the magnetic $NiSO_4/\gamma$-$Al_2O_3$ catalysts with different nickel contents; (c) DTA curves of magnetic $NiSO_4/\gamma$-$Al_2O_3$ catalysts with different nickel contents.**

[Color figure can be viewed in the online issue, which is available at www.interscience.wiley.com.]

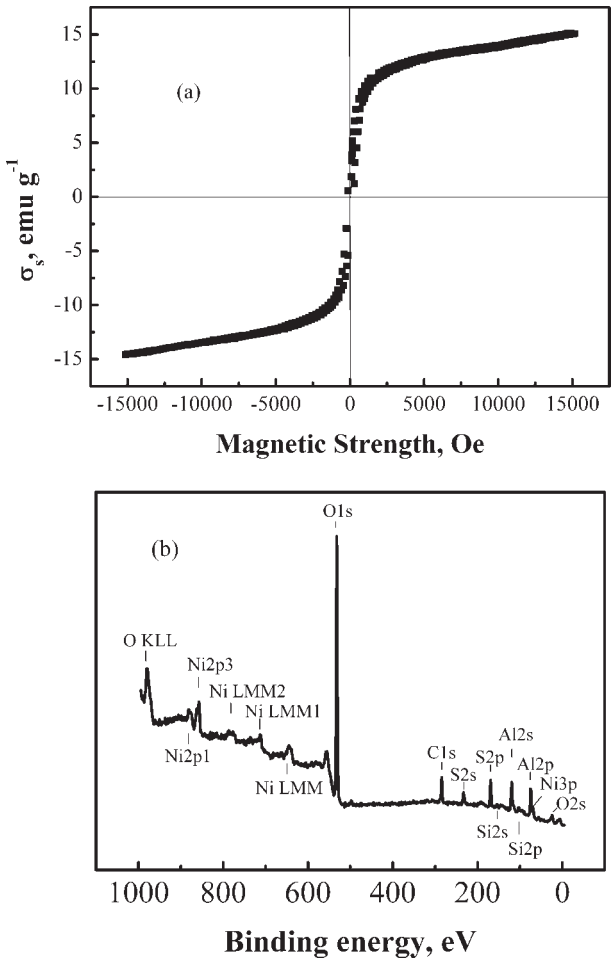


**Figure 3. (a) Hysteresis loop of the magnetic $NiSO_4/\gamma$-$Al_2O_3$ -7 catalyst; (b) XPS spectra of the magnetic $NiSO_4/\gamma$-$Al_2O_3$ -7 catalyst.**

ture (around 413 K) similar to the lowest temperature peak observed for $NiSO_4 \cdot 6H_2O$. When the nickel content was as low as 4.0 % (wt), no other peaks appeared in the temperature range 423–1173 K. As the nickel content was increased to 7.0% (wt), a very weak peak at 1093 K was observed, whilst two weak peaks located at 1033 K and 1107 K were observed for the $NiSO_4/\gamma$-$Al_2O_3$ -10catalyst. These data suggest that the decomposition of sulfate anions is affected by the presence of the $\gamma$-$Al_2O_3$ support. The significant difference between the DTA trace of the material with a nickel content of 10.0% (wt) and those of materials with lower nickel contents is consistent with the XRD and $NH_3$-TPD results, which suggested that a monolayer dispersion was obtained when the nickel loading was not higher than 8.0% (wt).

Figure 3a shows the hysteresis loop of the magnetic $NiSO_4/\gamma$-$Al_2O_3$-7 catalyst. The specific saturation magnetization of the sample was 15.0 emu g$^{-1}$, which is higher than that of other reported magnetic solid acid catalysts.[32,33]

Figure 3b shows the XPS spectra of the magnetic $NiSO_4/\gamma$-$Al_2O_3$-7 catalyst. According to the X-ray fluorescence results, the catalyst contained 20.9 % (wt) $Fe_3O_4$, however, it could be seen from the XPS spectra that there was no Fe element on the surface of the catalyst. The result indicates that the $SiO_2$ shell on the surface of $Fe_3O_4$ particles is dense and uniform which can prevent the $Fe_3O_4$ particles from affecting the performance of the catalyst.

### *Light FCC gasoline olefin oligomerization over the magnetic $NiSO_4/\gamma$-$Al_2O_3$ catalysts in the fixed-bed reactor*

Magnetic $NiSO_4/\gamma$-$Al_2O_3$ catalysts with different nickel contents were assessed for olefin oligomerization performance in the fixed-bed reactor. Figure 4 shows the variation in diesel yield as a function of nickel content obtained with magnetic $NiSO_4/\gamma$-$Al_2O_3$ catalysts calcined at 773 K. The diesel yield increased with nickel content up to 7.0% (wt), and then decreased at higher nickel contents. This is consistent with maximum number of acid sites being present in the material with a nickel content of 7.0% (wt) (as discussed above and shown in Supp. Info. Figure 1).

The magnetic catalyst with a nickel loading of 7.0% (wt), $NiSO_4/\gamma$-$Al_2O_3$-7, was calcined at different temperatures and its efficacy in olefin oligomeriation was assessed. As shown in Figure 5a, the $NiSO_4/\gamma$-$Al_2O_3$-7 catalyst calcined at 773 K afforded the maximum diesel yield, of about 40%. Figure 5b shows the $NH_3$-TPD curves of the magnetic $NiSO_4/\gamma$-$Al_2O_3$-7 catalyst calcined at different temperatures. Each curve showed two peaks, one at 463 K corresponding to $NH_3$ desorption from weak acid sites, and the other at about 553 K corresponding to desorption from moderate strength acid sites. The relative intensities of these two peaks varied as the calcination temperature was increased from 673 to 973 K. For a calcination temperature of 773 K, the number of moderate strength acid sites was larger than that of the number of weak acid sites. Furthermore, the amount of $NH_3$ adsorbed on the catalyst calcined at 773 K, 14.5 ml g$^{-1}$, was larger than that adsorbed on the catalysts calcined at higher or lower temperatures (see Supp. Info. Figure 2).

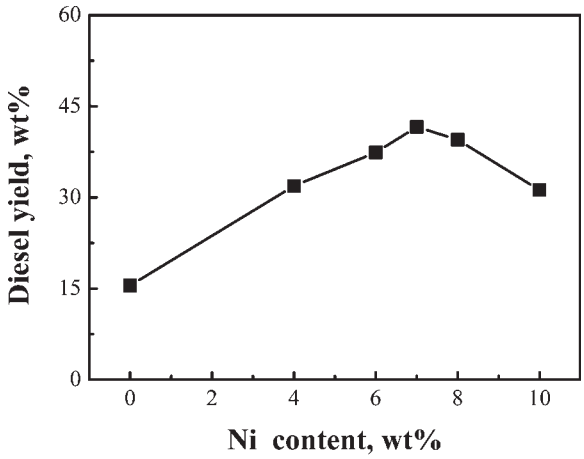


**Figure 4. Effect of varying nickel content on the diesel yield over magnetic $NiSO_4/\gamma$-$Al_2O_3$ catalysts in a fixed-bed reactor operated under the conditions of temperature of 463 K, pressure of 3.0 MPa, and LHSV of 1.0 h$^{-1}$.**

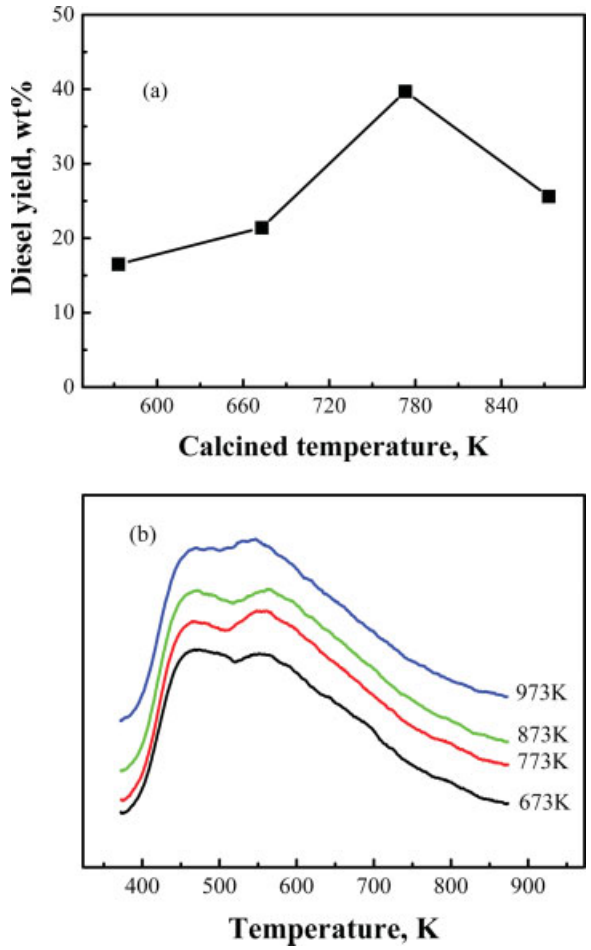


**Figure 5. (a) Effect of varying calcination temperature of the catalyst on the diesel yield over the magnetic $NiSO_4/\gamma$-$Al_2O_3$ catalyst in a fixed-bed reactor operated under the conditions of temperature of 463 K, pressure of 3.0 MPa, and LHSV of 1.0 $h^{-1}$; (b) $NH_3$-TPD curves of the magnetic $NiSO_4/\gamma$-$Al_2O_3$ catalyst calcined at different temperature.**

[Color figure can be viewed in the online issue, which is available at www.interscience.wiley.com.]

The aforementioned data suggest that the maximum activity of the magnetic catalyst can be obtained with a nickel loading of 7.0% (wt) when calcined at 773 K, since this material has a monolayer of active catalyst on the support, with the maximum number of medium strength acidic sites. Therefore this catalyst was selected for further studies in the fixed-bed and MSB reactors.

### *Light FCC gasoline olefin oligomerization intensified by the MSB reactor*

Figure 6 shows a comparison of the effects of varying reaction temperature, pressure, space velocity and magnetic field intensity on the diesel yield for both fixed-bed and MSB reactors incorporating the magnetic $NiSO_4/\gamma$-$Al_2O_3$ -7 catalyst which had been calcined at 773 K.

Figure 6a shows the diesel yield as a function of varying temperature under the reaction conditions of pressure of 3.0 MPa and an LHSV of 1.0 $h^{-1}$ in the fixed-bed reactor and with pressure 3.0 MPa, LHSV of 4.0 $h^{-1}$ and magnetic field intensity of 30 kA $m^{-1}$ in the MSB reactor. It can be seen that the optimal reaction temperatures were 443 and 463 K for the MSB and the fixed-bed reactors, respectively. The diesel yield obtained using the MSB reactor was higher than that obtained with the fixed-bed reactor over the entire temperature range from 423 to 503 K. This can be attributed to the MSB having more efficient interphase mass transfer properties, lower pressure drop, and the absence of particle clogging, which inhibits formation of hotspots during the exothermic reaction system allowing a lower optimal reaction temperature.[25,27]

Figure 6b shows the effect of varying the system pressure on the oligomerization performance of the magnetic catalyst under the reaction conditions of temperature of 463 K and LHSV of 1.0 $h^{-1}$ in the fixed-bed reactor and temperature of 443 K, LHSV of 4.0 $h^{-1}$ and magnetic field intensity of 30 kA $m^{-1}$ in the MSB reactor. The diesel yield showed a gradual increase with system pressure in both reactors. At low pressures, the light FCC gasoline feed was partially gasified in the reactor so that lower diesel yield was obtained. Increasing the system pressure resulted in liquefying of the feed, which led to the observed increased diesel yields.

Figure 6c shows the influence of varying LHSV on the diesel yield under the reaction conditions of temperature of 463 K and pressure of 3.0 MPa in both reactors and magnetic field intensity of 30 kA $m^{-1}$ in the MSB reactor. In the fixed-bed reactor, the diesel yield decreased sharply from 41.6% (wt) to 23.1% (wt) as the LHSV was increased from 1.0 to 4.0 $h^{-1}$. In contrast, in the MSB reactor the diesel yield showed only a gradual decrease from 45.6 to 39.7% (wt) when the LHSV was increased from 2.0 to 6.0 $h^{-1}$, whilst even for a much higher LHSV of 8.0 $h^{-1}$ the diesel yield only decreased to 33.3% (wt).

High space velocities shorten the contact time of the feed with the catalyst in the fixed-bed reactor, which results in the observed decrease in the diesel yield. In the MSB reactor, however, the catalyst bed expands with increasing space velocity, and the contact time is not reduced as sharply as that in the fixed-bed reactor, and consequently the diesel yield is relatively stable over a broad range of space velocities. The ability to use higher space velocities highlights the superior performance of the MSB reactor compared with the fixed-bed reactor.

Figure 6d shows the effect on the diesel yield of varying the magnetic field intensity in the MSB reactor under the conditions of temperature of 443 K, pressure of 3.0 MPa and LHSV of 6.0 $h^{-1}$. As the magnetic field intensity was increased from 10.0 to 30.0 kA $m^{-1}$, the diesel yield increased from 28.4 to 41.2% (wt), and then remained almost constant with a further increase in magnetic field intensity to 40.0 kA $m^{-1}$. The optimal magnetic field intensity is therefore 30.0–40.0 kA $m^{-1}$.

This dependence of diesel yield on the magnetic field intensity can be attributed to the hydrodynamic characteristics of the MSB reactor. It is known that when the liquid velocity is greater than the minimum fluidization velocity, the MSB has three different operating regimes depending on the magnetic field intensity.[39] These are the particulate regime, the chain regime, and the magnetically condensed regime,

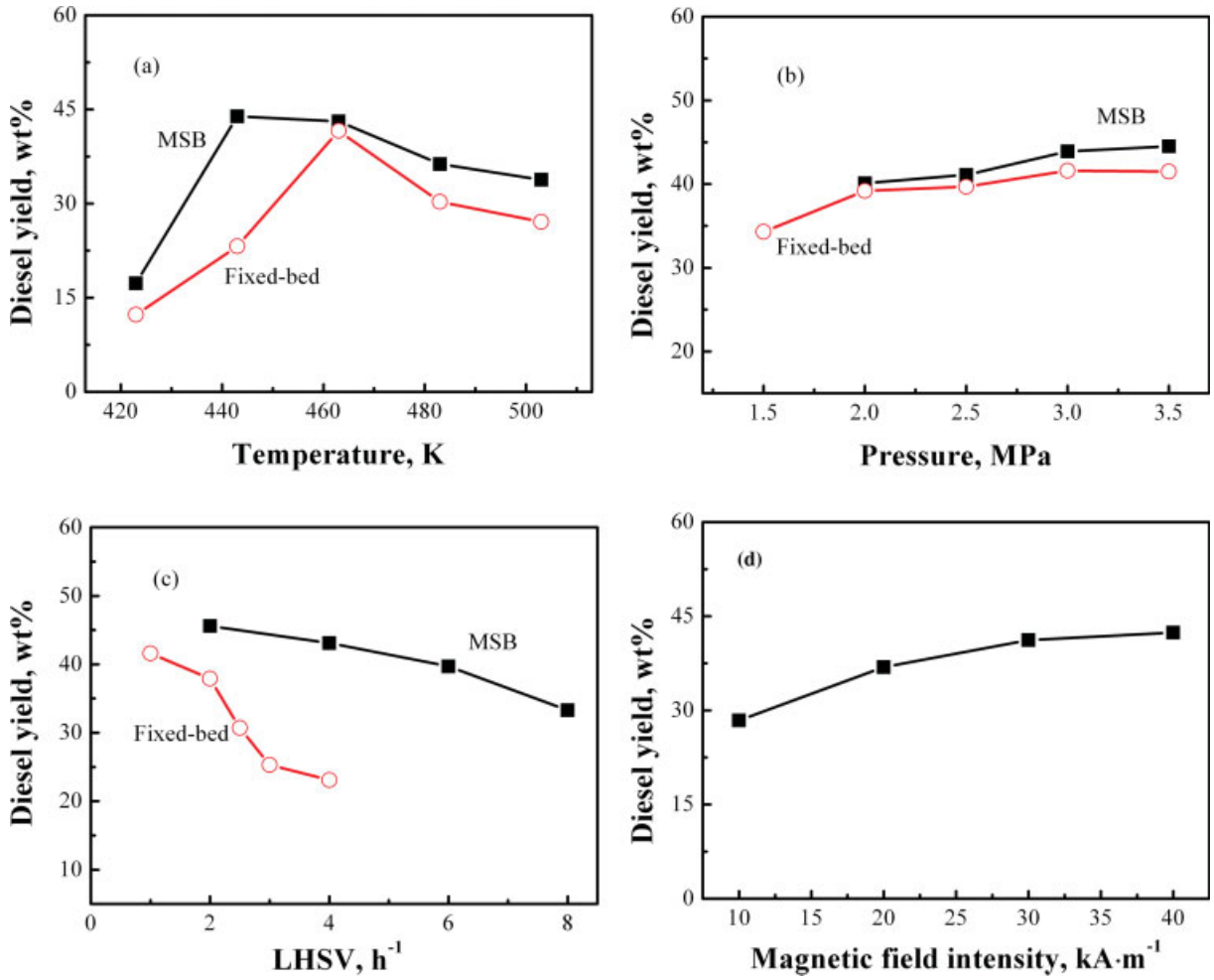


**Figure 6. Oligomerization performance of the magnetic $NiSO_4/\gamma$-$Al_2O_3$ -7catalyst calcined at 773 K in fixed-bed and MSB reactors as a function of: (a) varying reaction temperature under the conditions of pressure of 3.0 MPa, and LHSV of 1.0 $h^{-1}$ for the fixed-bed reactor and pressure of 3.0 MPa, LHSV of 4.0 $h^{-1}$, and magnetic field intensity of 30 kA $m^{-1}$ for the MSB reactor; (b) varying system pressure under the conditions of temperature of 463 K, and LHSV of 1.0 $h^{-1}$ for the fixed-bed reactor and temperature of 443 K, LHSV of 4.0 $h^{-1}$, and magnetic field intensity of 30 kA $m^{-1}$ for the MSB reactor; (c) varying LHSV under the conditions of temperature of 463 K, and pressure of 3.0 MPa for the fixed-bed reactor and temperature of 463 K, pressure of 3.0 MPa, and magnetic field intensity of 30 kA $m^{-1}$ for the MSB reactor; (d) varying magnetic field intensity under the conditions of temperature of 443 K, pressure of 3.0 MPa, and LHSV of 6.0 $h^{-1}$ in the MSB reactor.**

[Color figure can be viewed in the online issue, which is available at www.interscience.wiley.com.]

respectively. In the particulate regime, the catalysts move freely, and backmixing and entrainment occur; in the chain regime, the catalyst particles align themselves along the direction of magnetic field, and the bed is operated in a stable state with uniform voidage; in the magnetically condensed regime, bypassing occurs and the surface of the catalyst is not fully available to the feed. Figure 7 shows the operation regimes with the different fluid velocity of light FCC gasoline in the MSB reactor. In case of the light FCC gasoline olefin oligomerization, magnetic field strengths in the range 30.0–40.0 kA $m^{-1}$ are sufficient to achieve chain regime operation in the MSB reactor, resulting in higher diesel yields, whereas at lower magnetic field strengths the particulate regime occurs resulting in lower diesel yields.

### *Comparisons of the results in the MSB and the fixed- bed reactors*

Based on the above experimental results, the ranges of optimal reaction conditions in the fixed-bed and the MSB reactors for light FCC gasoline olefin oligomerization are listed in Table 2. Table 3 shows the distillate range of the products obtained under the conditions of temperature 463 K, pressure of 3.0 MPa and LHSV of 1.0 for the fixed bed reactor and temperature of 443 K, pressure of 3.0 MPa, LHSV of 6.0 $h^{-1}$ and magnetic field intensity of 30.0 kA $m^{-1}$ for the MSB reactor. Although the average diesel yields in the MSB reactor were only slightly higher than those in the fixed-bed reactor, the broad space velocity range possible in the MSB indicates its excellent operational flexibility.

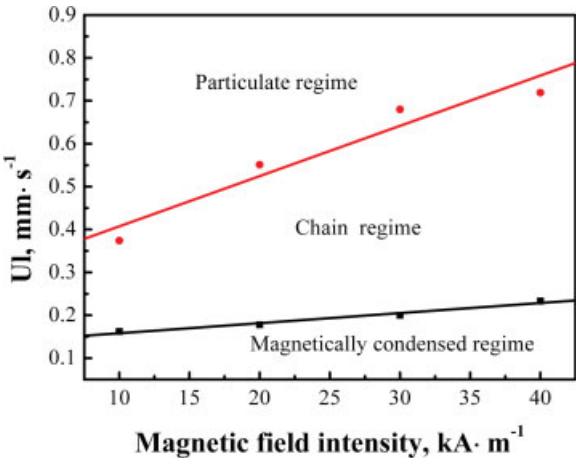


**Figure 7. The operation regimes under different fluid velocity of light FCC gasoline in the MSB reactor.**

[Color figure can be viewed in the online issue, which is available at www.interscience.wiley.com.]

### *Properties of the oligomerization products obtained in the MSB reactor*

Stability tests of the magnetic catalyst were performed in the MSB reactor for 100 h under the conditions of temperature of 443 K, pressure of 3.0 MPa, LHSV of 6.0 $h^{-1}$ and magnetic field intensity of 30.0 kA $m^{-1}$. The properties of the oligomerization products are given in Table 4. The gasoline distillate contains large quantities of light distillate and saturated hydrocarbons, making it a high-quality feed, after hydrogenation, for production of ethylene. Furthermore, the diesel distillate possesses a high cetane number and good low-temperature flow property and the characteristics of clean diesel, i.e. sulfur-free and containing a low content of aromatics. It should be noted that this diesel distillate meets the requirement of the GB 252-94 standards for $-50^{\#}$ diesel.

## Conclusions

High magnetic $NiSO_4/\gamma$-$Al_2O_3$ catalysts have been successfully prepared by impregnation of a $\gamma$-$Al_2O_3$ support containing a magnetic material of $Fe_3O_4$ with $NiSO_4$ solutions. Characterization by XRD, $NH_3$-TPD, and thermal analysis indicated that the magnetic $NiSO_4/\gamma$-$Al_2O_3$ catalyst with a nickel content of 7.0% (wt) had a monolayer dispersion of $NiSO_4$ and the largest number of moderate strength acid sites. This material also had a high specific saturation magnetization of 15.0 emu $g^{-1}$.

**Table 2. Range of Optimal Reaction Conditions in the MSB and the Fixed-bed Reactors with the Magnetic $NiSO_4/\gamma$-$Al_2O_3$ Catalyst**

| Items | MSB | Fixed-bed |
|---|---|---|
| Reaction temperature (K) | 443–463 | 463 |
| System pressure (MPa) | 3.0 | 3.0 |
| LHSV ($h^{-1}$) | 2.0–6.0 | 1.0–2.0 |
| Magnetic field intensity (kA $m^{-1}$) | 30.0 | – |
| Diesel yield (wt) % | 39.7–45.6 | 37.9–41.6 |

**Table 3. Distillate Range of the Product Obtained in the MSB and the Fixed-Bed Reactors with the Magnetic $NiSO_4/\gamma$-$Al_2O_3$ Catalyst**

| Distillate range (K) | MSB | Fixed-bed |
|---|---|---|
| Initial boiling point | 318 | 324 |
| 10% | 329 | 331 |
| 30% | 351 | 350 |
| 50% | 408 | 400 |
| 70% | 487 | 502 |
| 90% | 529 | 546 |
| Final boiling point | 601 | 618 |

Reaction Conditions: temperature of 443 K, pressure of 3.0 MPa, LHSV of 6.0 $h^{-1}$, and magnetic field intensity of 30 kA $m^{-1}$ for the MSB reactor, and temperature of 463 K, pressure of 3.0 MPa and LHSV of 1.0 $h^{-1}$ for the fixed-bed reactor.

The magnetic $NiSO_4/\gamma$-$Al_2O_3$-7 material with a nickel content of 7.0% (wt) was assessed as a light FCC gasoline olefin oligomerization catalyst in both fixed-bed and MSB reactors. In the fixed-bed reactor, the optimal reaction conditions were found to be a temperature of 463 K, pressure of 3.0 MPa and LHSV of 1.0–2.0 $h^{-1}$, under which conditions the diesel yield was in the range 37.9–41.6% (wt). In the MSB reactor with a magnetic field strength of 30.0–40.0 kA $m^{-1}$, the optimal reaction temperature was reduced to 443 K, and space velocities over a broad range of 2.0–6.0 $h^{-1}$ resulted in higher diesel yields than those obtainable in the fixed-bed reactor.

A stability test of the magnetic $NiSO_4/\gamma$-$Al_2O_3$-7 catalyst with a nickel content of 7.0% (wt) was performed under the conditions of temperature of 443 K, pressure of 3.0 MPa, LHSV of 6.0 $h^{-1}$ and magnetic field strength of 30.0 kA $m^{-1}$ in the MSB reactor for 100 h. The resulting products comprised a gasoline distillate that is a suitable raw material for ethylene production, and a clean diesel distillate that pos-

**Table 4. Properties of the Oligomerization Products**

| | | |
|---|---|---|
| Gasoline distillate | Density (293 K), g/$cm^3$ | 0.658 |
| | Distillate range (K) | |
| | Initial boiling point | 312 |
| | 50% | 346 |
| | 90% | 414 |
| | 95% | 433 |
| | Final boiling point | 443 |
| | Group compositions (wt) % | |
| | Saturated hydrocarbon | 74.8 |
| | Olefin | 22.9 |
| | Aromatic hydrocarbon | 2.3 |
| Diesel distillate | Density (293 K), g/$cm^3$ | 0.80 |
| | Kinematic viscosity (293 K), $mm^2/s$ | 3.87 |
| | Distillate range (K) | |
| | Initial boiling point | 443 |
| | 50% | 506 |
| | 90% | 616 |
| | 95% | 633 |
| | Final boiling point | 639 |
| | Freezing point (K) | <-323 |
| | Closed-flash point (K) | 335 |
| | Mechanical impurity | null |
| | Sulfur content | 0 |
| | Colority | 0.5 |
| | Cetane number | 60 |
| | Hydrocarbon composition (wt) % | |
| | Alkane | 34.70 |
| | Cycloalkane | 61.10 |
| | Alkylbenzene | 4.20 |

sesses high cetane number and good low temperature flow properties, meeting the requirements of GC252-94 standards for -50# diesel. The results show that the MSB reactor containing the magnetic $NiSO_4/\gamma$-$Al_2O_3$ catalyst allows a significant intensification of the light FCC gasoline olefin oligomerization process by enhancing the interphase mass transfer and the operational flexibility.

## Acknowledgments

This work was supported by the National Basic Research Program of China (2006CB202500) and NSFC (20676096).

## Notation

LHSV = liquid hourly space velocity, ($h^{-1}$)
$\sigma_s$ = specific saturation magnetization, (emu $g^{-1}$)
Ul = the fluid velocity of light FCC gasoline, (mm $s^{-1}$)

## Literature Cited

1. Jamieson A, McManus G. GTL production will partially ease regional diesel, naphtha imbalances. *Oil Gas J*. 2007;105:49–53.
2. Wu K, Fesharaki F. As oil demand surges, China adds and expands refineries. *Oil Gas J*. 2005;103:20–23.
3. Qian EW. Development of novel nonhydrogenation desulfurization process-oxidative desulfurization of distillate. *J Jpn Petrol Inst*. 2008;51:14–31.
4. Catani R, Mandreoli M, Rossini S, Vaccari A. Mesoporous catalysts for the synthesis of clean diesel fuels by oligomerisation of olefins. *Catal Today*. 2002;75:125–131.
5. Flego C, Marchionna M, Perego C. High quality diesel by olefin oligomerisation: new tailored catalysts. *Stud Surf Sci Catal*. 2005;158: 1271–1278.
6. Klerk AD. Oligomerization of 1-hexene and 1-octene over solid acid catalysts. *Ind Eng Chem Res*. 2005;44:3887–3893.
7. Heveling J, Nicolaides CP, Scurrell MS. Cayalysts and conditions for the highly efficient, selective and stable heterogeneous oligomerization of ethylene. *Appl Catal A: Gen*. 1998;173:1–9.
8. Tabak SA, Krambeck FJ, Garwood WE. Conversion of propylene and butylenes over ZSM-5 catalyst. *AIChE J*. 1986;32:1526–1531.
9. Quann RJ, Green LA, Tabak SA, Krambeck FJ. Chemistry of olefin oligomerization over ZSM-5 catalyst. *Ind Eng Chem Res*. 1988;27: 565–570.
10. Klerk A de. Properties of synthetic fuels from h-zsm-5 oligomerization of fischer-tropsch type feed materials. *Energy Fuels*. 2007;21: 3084–3089.
11. Nkosi B, Ng FTT, Rempel GL. The oligomerization of 1-butene using NaY zeolites ion-exchanged with different nickel precursor salts. *Appl Catal A: Gen*. 1997;161:153–166.
12. Nkosi B, Ng FTT, Rempel GL. The oligomerization of butane with partially alkali changed NiNaY zeolite catalysts. *Appl Catal A: Gen*. 1997;158:225–241.
13. Chiche B, Sauvage E, Di Renzo F, Ivanova II, Fajula F. Butene oligomerization over mesoporous MTS-type aluminosilicates. *J Mol Catal A: Chem*. 1998;134:145–157.
14. Heveling J, Nicolaides CP, Scurrell M. Activity and selectivity of nickel-exchanged silica-alumina catalysts for the oligomerization of propene and 1-butene into distillate-range products. *Appl Catal A: Gen*. 2003;248:239–248.
15. Coetzee JH, Mashapa TN, Prinsloo NM, Rademan JD. An improved solid phosphoric acid catalyst for alkene oligomerization in a Fischer-Tropsch refinery. *Appl Catal A: Gen*. 2006;308:204–209.
16. Klerk A de. Distillate production by oligomerization of Fischer-Tropsch olefins over solid phosphoric acid. *Energy Fuels*. 2006;20: 439–445.
17. Arata K, Hino M, Yamagata N. Acidity and catalytic activity of zirconium and titanium sulfate heat-treated at high temperature. Solid superacid catalysts. *Bull Chem Soc Jpn*. 1990;63: 244–246.
18. Tanabe K, Misono M, Ono Y, Hattori H. New solid acids and bases. *Stu Surf Sci Catal*. 1989;51:185–186.
19. Cai TX. Studies of a new alkene oligomerization catalyst derived from nickel sulfate. *Catal Today*. 1999;51:153–160.
20. Cai TX, Cao DX, Song ZY, Li LH. Catalytic behavior of $NiSO_4/\gamma$-$Al_2O_3$ for ethylene dimerization. *Appl Catal A: Gen*. 1993;95:L1–L7.
21. Sohn JR, Park WC. The roles of active sites of nickel sulfate supported on $\gamma$-$Al_2O_3$ for ethylene dimerization. *Appl Catal A: Gen*. 2003;239:269–278.
22. Sohn JR, Park WC, Kim HW. Characterization of nickel sulfate supported on $\gamma$-$Al_2O_3$ for ethylene dimerization and its relationship to acidic properties. *J Catal*. 2002;209:69–74.
23. Sohn JR, Park WC. Nickel sulfate supported on $\gamma$-$Al_2O_3$ for ethylene dimerization. *J Mol Catal A: Chem*. 1998;133:297–301.
24. Sohn JR, Lim JS. Ethylene dimerization over $NiSO_4$ supported on $Fe_2O_3$-promoted $ZrO_2$ catalyst. *Catal Today*. 2006;111:403–411.
25. Hristov J. Magnetic field assisted fluidization: a unified approach, part 5: a hydrodynamic treatise on liquid-solid fluidized beds. *Rev Chem Eng*. 2006;22:195–375.
26. Hristov J. Magnetic field assisted fluidization: a unified approach, part 2: solids batch gas-fluidized beds: versions and rheology. *Rev Chem Eng*. 2003;19:1–132.
27. Hristov J. Magnetic field assisted fluidization: a unified approach, part 6: topics of gas-liquid-solid fluidized bed hydrodynamics. *Rev Chem Eng*. 2007;23:373–526.
28. Li W, Zong BN, Li XF, Meng XK, Zhang JL. Interphase mass transfer in G-L-S magnetically stabilized bed with amorphous alloy SRNA-4 catalyst. *Chin J Chem Eng*. 2006;14:734–739.
29. Webb C, Kang HK, Moffat G, Williams RA, Estévez AM, Cuéllar J, Jaraiz E, Galán MA. The magnetically stabilized fluidized bed bioreactor: a tool for improved mass transfer in immobilized enzyme systems? *Chem Eng J*. 1996;61:241–246.
30. Meng XK, Mu XH, Zong BN, Min EZ, Zhu ZH, Fu SB, Luo YB. Purification of caprolactam in magnetically stabilized bed reactor. *Catal Today*. 2003;79–80:21–27.
31. Pan ZY, Dong MH, Meng XK, Zhang XX, Mu XH, Zong BN. Integration of magnetically stabilized bed and amorphous nickel alloy catalyst for CO methanation. *Chem Eng Sci*. 2007;62:2712–2717.
32. Dong MH, Pan ZY, Pen Y, Meng XK, Mu XH, Zong BN, Zhang JL. Selective acetylene hydrogenation over core-shell magnetic Pd-supported catalysts in a magnetically stabilized bed. *AIChE J*. 2008;54:1358–1364.
33. Yang PP, Wang J, Shang YC, Yang JJ. Synthesis, characterization and catalytic performance of a novel magnetic $SO_4^{2-}$-$Y_2O_3$-$Fe_3O_4$-$ZrO_2$ solid acid catalyst. *React Kinet Catal Lett*. 2008;93:85–92.
34. Wang J, Yang PP, Fan MQ, Yu W, Jing XY, Zhang ML, Duan X. Preparation and characterization of novel magnetic $ZrO_2/TiO_2/Fe_3O_4$ solid superacid. *Mater Lett*. 2007;61:2235–2238.
35. Feng JT, Lin YJ, Li F, Evan DG, Li DQ. Preparation, structure and properties of micro-spherical alumina with magnetic spinel ferrite cores. *Appl Catal A: Gen*. 2007;329:112–119.
36. Deng YH, Qi DW, Deng CH, Zhang XM, Zhao DY. Superparamagnetic high-magnetization microspheres with an $Fe_3O_4$@$SiO_2$ core and perpendicularly aligned mesoporous $SiO_2$ shell for removal of microcrytins. *J Am Chem Soc*. 2008;130:28–29.
37. Castano P, Pawelec B, Fierro JLG, Arandes JM, Bilbao J. Enhancement of pyrolysis gasoline hydrogenation over Pd-promoted Ni/$SiO_2$-$Al_2O_3$ catalysts. *Fuel*. 2007;86:2262–2274.
38. Siriwardane RV, Poston JA Jr, Fisher EP, Shen MS, Miltz AL. Decomposition of the sulfates of copper, iron (II), iron (III), nickel, and zinc: XPS, SEM, DRIFTS, XRD, and TGA study. *Appl Surf Sci*. 1999;152:219–136.
39. Meng XK, Mu XH, Jiang YS, Zong BN, Min EZ, Li BX, Zhu HJ, Chen XB, Fu SB, Zhu ZH. Hydrodynamic behavior of liquid-solid magnetically stabilized bed. *J Chem Ind Eng*. 2004;55:134–137 (in Chinese).

*Manuscript received May 19, 2008, and revision received Sept. 3, 2008.*